

Green's function approach to interacting lattice polaritons and optical nonlinearities in subwavelength arrays of quantum emitters

Simon Panyella Pedersen*, Georg M. Bruun†, and Thomas Pohl*

* *Institute for Theoretical Physics, TU Wien, Wiedner Hauptstraße 8-10/136, A-1040 Vienna, Austria and*

† *Department of Physics and Astronomy, Aarhus University, DK-8000 Aarhus C, Denmark*

(Dated: June 18, 2024)

Sub-wavelength arrays of quantum emitters offer an efficient free-space approach to coherent light-matter interfacing, using ultracold atoms or two-dimensional solid-state quantum materials. The combination of collectively suppressed photon-losses and emerging optical nonlinearities due to strong photon-coupling to mesoscopic numbers of emitters holds promise for generating nonclassical light and engineering effective interactions between freely propagating photons. While most studies have thus far relied on numerical simulations, we describe here a diagrammatic Green's function approach that permits analytical investigations of nonlinear processes. We illustrate the method by deriving a simple expression for the scattering matrix that describes photon-photon interactions in an extended two-dimensional array of quantum emitters, and reproduces the results of numerical simulations of coherently driven arrays. The approach yields intuitive insights into the nonlinear response of the system and offers a promising framework for a systematic development of a theory for interacting photons and many-body effects on collective radiance in two-dimensional arrays of quantum emitters.

Recent progress in controlling quantum many-body systems opens up new ways to engineer light-matter interfaces, in which freely propagating photons can be coupled strongly to assemblies of quantum emitters [1–12]. For example, the trapping of atoms in optical lattices [13] or the confinement of semiconductor excitons in moiré lattices of two-dimensional materials [14–16] makes it possible to create regular arrays of saturable quantum emitters with subwavelength lattice spacing. Importantly, the collective interaction of light with such quantum optical metasurfaces allows one to inhibit photon-scattering losses while generating strong mode-selective coupling to an incident light field [17–19]. This was demonstrated in experiments with ultracold atoms in optical lattices [1] and holds promise for applications, from enhancing the efficiency of optical quantum memories [20–23], coherent wavefront shaping [24–27], to the generation and manipulation of nonclassical states of light [28–33].

The system can be described within a Markov approximation that permits integrating out the photonic degrees of freedom and yields an effective Lindblad master equation for the many-body dynamics of the quantum emitters [18–33]. The Markovian master equation can be solved numerically for a few incident photons to obtain the optical response of the emitters by recovering the underlying photonic dynamics from an input-output relation for the light field.

In this paper, we discuss a different approach that permits an analytic treatment of emerging photon correlations by considering nonlinear optical processes within a scattering formalism. Here, one employs a polariton picture in terms of dressed photons and dressed excitations that finds broad application in optics, from semiconductor microcavities [34], to light-propagation in continuous optical media or discrete chains of emitters [35]. Describing the dynamics in terms of time-dependent Green's

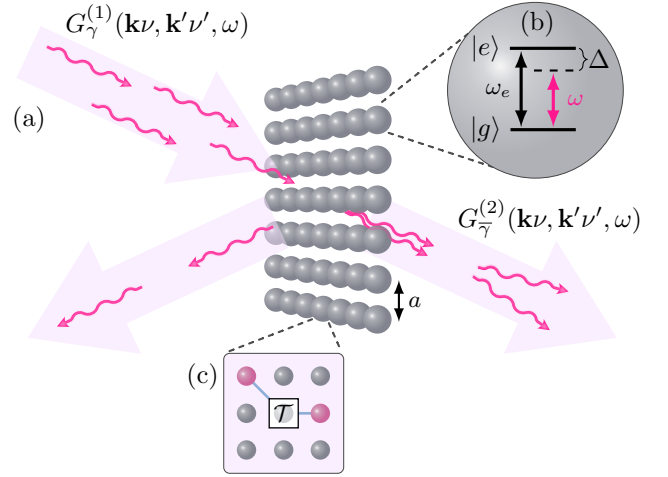


Figure 1. (a) Illustration of the considered setup, whereby incident photons interact with a 2D array of two-level quantum emitters, depicted in panel (b). Saturation of the two-level emitters generates photon-photon interactions that can be described by (c) a scattering \mathcal{T} -matrix for photon-dressed emitter excitations and a two-photon propagator $G_{\vec{\gamma}}^{(2)}$. Scattering leads to the correlated transmission of bound photon-pairs, which causes bunching as well as antibunching of the emitted light.

functions, our method does generally not rely on the Markovian approximation but recovers the results of the master equation in the Markovian limit. Treating the emitters as a lattice of hardcore bosons yields dressed propagators for polaritonic excitations of the array, from which one can obtain effective polariton interactions in terms of a scattering matrix that describes the correlated collective emission of photons. We illustrate the method by deriving analytical and intuitive expressions for the scattering of two incident photons. Moreover,

we show that the method yields a simple expression for spatio-temporal photon correlations that agrees remarkably well with the numerical simulation of the effective master equation and reveals the emergence of a two-photon bound state, explaining the specific form of the observed temporal photonic pair-correlations. Our approach thus yields intuitive insights into the leading-order nonlinear response of quantum-emitter arrays and provides a powerful framework for developing a systematic description of many-body effects [36–38] regarding effective photon interactions and collective radiance in extended arrays of quantum emitters.

I. THE SYSTEM

Figure 1 illustrates the considered system, which consists of N two-level emitters that are arranged in a two-dimensional array with a lattice spacing a in the xy -plane at $z = 0$. The system is described by the Hamiltonian

$$H = \sum_n \omega_e \hat{\sigma}_n^\dagger \hat{\sigma}_n + \sum_{\mathbf{k}, \nu} \omega_{\mathbf{k}} \hat{b}_{\mathbf{k}\nu}^\dagger \hat{b}_{\mathbf{k}\nu} + \sum_{n, \mathbf{k}, \nu} \left(\bar{g}_{\mathbf{k}\nu} e^{-i\mathbf{k}\cdot\mathbf{r}_n} \hat{b}_{\mathbf{k}\nu}^\dagger \hat{\sigma}_n + \text{H.c.} \right), \quad (1)$$

where the raising and lowering operators, $\hat{\sigma}_n^\dagger = |e_n\rangle\langle g_n|$ and $\hat{\sigma}_n$, are defined by the ground state $|g_n\rangle$ and excited state $|e_n\rangle$ of the n 'th emitter, and $\omega_e = 2\pi c/\lambda_e$ denotes the corresponding transition frequency (c is the speed of light). While the first term, thus, describes the isolated dynamics of the two-level emitters, the second term captures the bare propagation of photons with the linear vacuum dispersion $\omega_{\mathbf{k}} = c|\mathbf{k}|$. The corresponding operator $\hat{b}_{\mathbf{k}\nu}$ annihilates photons with momentum \mathbf{k} and unit polarization vector $\hat{\mathbf{e}}_{\mathbf{k}\nu}$, labeled by the index ν . The third term in Eq. (1) accounts for the dipole coupling between emitters and photons, with a coupling strength $\bar{g}_{\mathbf{k}\nu} = i\sqrt{\omega_{\mathbf{k}}/2\hbar\epsilon_0 V} \hat{\mathbf{e}}_{\mathbf{k}\nu}^\dagger \mathbf{d}$, where V is a quantization volume for the photonic modes. To be specific, we assume here that the two-level emitters couple to right-circularly polarized light in the xy -plane of the array, such that the corresponding transition dipole moment can be written as $\mathbf{d} = d(1, i, 0)^T/\sqrt{2}$.

This system can be described within an input-output formalism [18–33] that focuses on the spin-dynamics of the emitters. Here, one integrates out the photonic degrees of freedom and applies a Markov approximation to express the total light field as

$$\hat{\mathbf{E}}(\mathbf{r}, t) = \hat{\mathbf{E}}^{(0)}(\mathbf{r}, t) + \mu_0 \omega_e^2 \sum_n \mathbf{G}(\mathbf{r}, \mathbf{r}', \omega_e) \mathbf{d} \hat{\sigma}_n(t), \quad (2)$$

where $\hat{\mathbf{E}}^{(0)}(\mathbf{r}, t) = \frac{i}{\sqrt{2\hbar\epsilon_0 V}} \sum_{\mathbf{k}, \nu} \sqrt{\omega_{\mathbf{k}}} \hat{\mathbf{e}}_{\mathbf{k}\nu} e^{i\mathbf{k}\cdot\mathbf{r}} \hat{b}_{\mathbf{k}\nu}^{(0)}$ is the bare electric field, expressed via the bare photon field, $\hat{b}_{\mathbf{k}\nu}^{(0)}$, in the absence of the emitters and the induced light field that is generated by them. The latter is determined

by the dyadic Green's function, $\mathbf{G}(\mathbf{r}, \mathbf{r}', \omega_e)$ of the free-space electromagnetic field [39]. This leads to a master equation for the emitters, with an effective Hamiltonian

$$\hat{H} = \sum_n \omega_e \hat{\sigma}_n^\dagger \hat{\sigma}_n + \sum_{n, \mathbf{k}, \nu} \left(\bar{g}_{\mathbf{k}\nu}^* e^{i\mathbf{k}\cdot\mathbf{r}_n} \hat{b}_{\mathbf{k}\nu}^{(0)} \hat{\sigma}_n^\dagger + \text{H.c.} \right) - \sum_{n \neq m} J_{mn} \hat{\sigma}_m^\dagger \hat{\sigma}_n, \quad (3)$$

and Lindbladian

$$\hat{\mathcal{L}}(\hat{\rho}) = \sum_{n, m} \Gamma_{mn} (2\hat{\sigma}_m \hat{\rho} \hat{\sigma}_n^\dagger - \{\hat{\sigma}_m^\dagger \hat{\sigma}_n, \hat{\rho}\}) \quad (4)$$

that describes the driven-dissipative dynamics of the density matrix $\hat{\rho}$ for the N -emitter system. The two-body terms result from photon-exchange between the emitters and are determined by $\frac{\mu_0 \omega_e^2}{\hbar} \mathbf{d}^\dagger \mathbf{G}(\mathbf{r}_m, \mathbf{r}_n, \omega_e) \mathbf{d} = J_{mn} + i\Gamma_{mn}$ [39]. This readily yields the linear optical response captured by the collective Lamb shift

$$\tilde{\Delta}_{\mathbf{k}_\perp} = N^{-1} \sum_{m \neq n} e^{i\mathbf{k}\cdot(\mathbf{r}_m - \mathbf{r}_n)} J_{mn}, \quad (5)$$

and collective linewidth

$$\tilde{\Gamma}_{\mathbf{k}_\perp} = N^{-1} \sum_{m, n} e^{i\mathbf{k}\cdot(\mathbf{r}_m - \mathbf{r}_n)} \Gamma_{mn} \quad (6)$$

of the system, which only depend on the two-dimensional transverse momentum, $\mathbf{k}_\perp = (k_x, k_y)$, since $z = 0$ in the plane of the array.

Here, we develop a different approach to analyze the system, which describes the nonlinear optical response in terms of quasiparticle scattering processes. To this end, we treat the excited emitter states with bosonic operators, $\hat{a}_n = \hat{\sigma}_n$, and introduce a repulsive onsite interaction term $\frac{U}{2} \sum_n \hat{a}_n^\dagger \hat{a}_n^\dagger \hat{a}_n \hat{a}_n$, which prevents double-excitation at a given site as $U \rightarrow \infty$ [40–44]. Next, we define bosonic momentum-space operators $\hat{a}_{\mathbf{k}_\perp} = a \sum_n e^{-i\mathbf{k}\cdot\mathbf{r}_n} \hat{a}_n$ for the emitters. Considering large lattices, one may take the limit $N \rightarrow \infty$ and $V \rightarrow \infty$ such that the Hamiltonian can be written as

$$H = \sum_\nu \int \frac{d^3 k}{(2\pi)^3} \omega_{\mathbf{k}} \hat{b}_{\mathbf{k}\nu}^\dagger \hat{b}_{\mathbf{k}\nu} + \int_{\text{BZ}} \frac{d^2 k_\perp}{(2\pi)^2} \omega_e \hat{a}_{\mathbf{k}_\perp}^\dagger \hat{a}_{\mathbf{k}_\perp} - \sum_\nu \int \frac{d^3 k}{(2\pi)^3} \left(g_{\mathbf{k}\nu} \hat{b}_{\mathbf{k}\nu}^\dagger \hat{a}_{\mathbf{k}_\perp} + \text{H.c.} \right) + \frac{U a^2}{2} \int_{\text{BZ}} \frac{d^2 k_\perp d^2 k'_\perp d^2 q_\perp}{(2\pi)^6} \hat{a}_{\mathbf{k}_\perp + \mathbf{q}_\perp}^\dagger \hat{a}_{\mathbf{k}'_\perp - \mathbf{q}_\perp}^\dagger \hat{a}_{\mathbf{k}_\perp} \hat{a}_{\mathbf{k}'_\perp}, \quad (7)$$

where $g_{\mathbf{k}\nu} = \sqrt{\omega_{\mathbf{k}}/2\hbar\epsilon_0 a^2} \hat{\mathbf{e}}_{\mathbf{k}\nu}^\dagger \mathbf{d}$. Note that the two-dimensional quasi-momentum of the excitations in the discrete array only takes on values within the first Brillouin zone (BZ) of the lattice, and $\hat{a}_{\mathbf{k}_\perp + \mathbf{q}_m} = \hat{a}_{\mathbf{k}_\perp}$ for any reciprocal lattice vector \mathbf{q}_m . As expressed by the

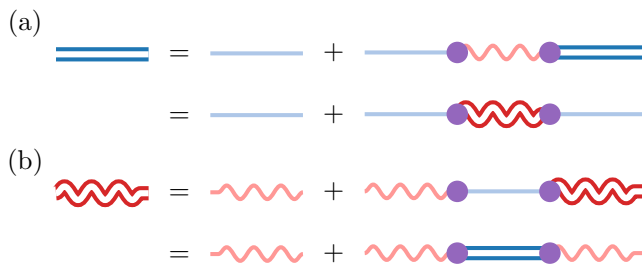


Figure 2. Depiction of the Dyson equation for (a) dressed emitter excitations, and (b) dressed photons. Single particle propagators are depicted as a single wavy or straight line for bare photons or bare excitations, while double lines indicate the dressed propagators due to the emitter-photon coupling (circular vertex). The relations can be recast as, respectively, shown in the second line.

third term in Eq. (7), identical modes of excited emitters can, hence, couple to different photonic modes, whose momenta differ by a reciprocal lattice vector in the xy -plane. This coupling leads to light scattering and photon losses out of the incident mode (Bragg scattering), but can be suppressed entirely in subwavelength lattices. The last term in Eq. (7), describes the effective onsite repulsion between emitter excitations. As this interaction is local and uniform it results in a momentum-independent scattering process that exchanges momenta between two modes, while conserving their total momentum. Below, we will exploit this simple form of the effective interaction to derive a compact description of the optical non-linearity of the array that emerges from saturation of the quantum emitters. We note, however, that the formalism presented here equally applies to other systems and can be straightforwardly used for extended range interactions such as dipolar or van der Waals interactions that appear in atomic [45, 46] or solid-state [8, 47–50] systems.

II. SINGLE-PHOTON DYNAMICS

Let us proceed by considering the single-excitation sector of Eq. (7), and illustrate the method by re-deriving the known linear optical response of the array. Specifically, we will recover the collective energy shift and decay rate, Eqs. (5) and (6), in the Markovian limit, and show how the dressed-photon propagator recovers the structure of the input-output relation given by Eq. (2).

From the first line in the momentum space Hamiltonian, Eq. (7), we can read off the bare propagator of the

emitter excitations

$$G_x^{(1)}(\mathbf{k}'_{\perp}, \mathbf{k}_{\perp}, \omega) = (2\pi)^2 \delta(\mathbf{k}'_{\perp} - \mathbf{k}_{\perp}) \mathcal{G}_x^{(1)}(\omega), \quad (8)$$

$$\mathcal{G}_x^{(1)}(\omega) = \frac{1}{\omega - \omega_e + i\eta},$$

as well as the bare photon propagator

$$G_{\gamma}^{(1)}(\mathbf{k}'_{\perp}, \mathbf{k}_{\perp}, \omega) = (2\pi)^3 \delta(\mathbf{k}' - \mathbf{k}) \delta_{\nu, \nu'} \mathcal{G}_{\gamma}^{(1)}(\mathbf{k}, \omega), \quad (9)$$

$$\mathcal{G}_{\gamma}^{(1)}(\mathbf{k}, \omega) = \frac{1}{\omega - \omega_{\mathbf{k}} + i\eta},$$

where η is a positive infinitesimal. The propagators, or Green's functions, of the bare excitations and photons are represented by a straight and wavy line, respectively, in the diagrams shown in Fig. 2. The light-matter coupling in the second line of Eq. (7) leads to a hybridization and yields single-particle propagators of dressed bosons corresponding to polaritons. The Green's functions of the corresponding quasiparticles are presented as straight (dressed excitations) and wavy (dressed photons) double lines in Fig. 2. The propagator for the dressed emitter excitations is obtained from the Dyson equation (Fig. 2a)

$$G_x^{(1)}(\mathbf{k}'_{\perp}, \mathbf{k}_{\perp}, \omega) = (2\pi)^2 \delta(\mathbf{k}'_{\perp} - \mathbf{k}_{\perp}) \mathcal{G}_x^{(1)}(\mathbf{k}_{\perp}, \omega) \quad (10)$$

$$\mathcal{G}_x^{(1)}(\mathbf{k}_{\perp}, \omega) = \frac{1}{\omega - \omega_a - \Sigma(\mathbf{k}_{\perp}, \omega) + i\eta}.$$

Using the expressions for the bare photon propagator $\mathcal{G}_{\gamma}^{(1)}$ and the light-matter coupling strength, $g_{\mathbf{k}\nu}$, we can obtain the self-energy illustrated in Fig. 2a as

$$\Sigma(\mathbf{k}_{\perp}, \omega) = \frac{1}{4\pi\hbar\epsilon_0 a^2} \sum_{\mathbf{q}_m} \int dk_z \frac{\omega_{\mathbf{k}} \mathbf{d}^{\dagger} \mathbf{Q} \mathbf{d}}{\omega - \omega_{\mathbf{k}} + i\eta}. \quad (11)$$

The projector $\mathbf{Q} = 1 - \hat{\mathbf{k}}\hat{\mathbf{k}}^{\dagger}$ into the plane of photon polarization vectors also defines the dyadic Green's function, \mathbf{G} , of the free-space electromagnetic field [22], which reveals the close connection to the input-output formalism, discussed in the preceding section. Indeed, one can rewrite Eq. (11) as (see Appendix A)

$$\Sigma(\mathbf{k}_{\perp}, \omega) = \frac{\mu_0 \omega_e^2}{\hbar} N^{-1} \sum_{m,n} e^{i\mathbf{k}\cdot(\mathbf{r}_m - \mathbf{r}_n)} \mathbf{d}^{\dagger} \mathbf{G}(\mathbf{r}_m, \mathbf{r}_n, \omega) \mathbf{d}. \quad (12)$$

By comparing with Eqs. (5) and (6), we see that the self-energy recovers the collective Lamb shift and decay rate of the array $\Sigma(\mathbf{k}_{\perp}, \omega_e) = \hat{\Delta}_{\mathbf{k}_{\perp}} - i\hat{\Gamma}_{\mathbf{k}_{\perp}}$.

The photon propagator cannot be readily calculated analogously, since the summation over reciprocal lattice vectors for the light-matter interaction complicates the direct solution of the Dyson equation shown Fig. 2b. However, diagrams in the expansion of the Dyson equation can be summed differently to recast the equation as shown in the second line of Fig. 2b. This yields the dressed-photon propagator

$$G_{\gamma}^{(1)}(\mathbf{k}\nu, \mathbf{k}'\nu', \omega) = G_{\gamma}^{(1)}(\mathbf{k}\nu, \mathbf{k}'\nu', \omega) + (2\pi)^2 \delta_{BZ}(\mathbf{k}'_{\perp} - \mathbf{k}_{\perp}) \mathcal{G}_{\gamma}^{(1)}(\mathbf{k}, \omega) g_{\mathbf{k}\nu} \mathcal{G}_{\bar{x}}^{(1)}(\mathbf{k}'_{\perp}, \omega) g_{\mathbf{k}'\nu'}^* \mathcal{G}_{\gamma}^{(1)}(\mathbf{k}', \omega) \quad (13)$$

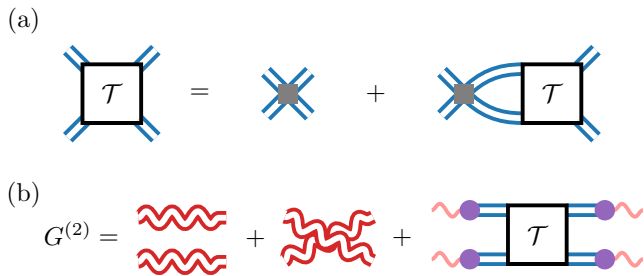


Figure 3. (a) The Bethe-Salpeter equation for the \mathcal{T} -matrix that describes interactions between dressed excitations due to the emitter saturation, as indicated by the square vertex. The two-photon propagator is depicted in panel (b).

in terms of the Green's function of the dressed emitter excitations, obtained from Eq. (10). Here

$$\delta_{BZ}(\mathbf{k}'_{\perp} - \mathbf{k}_{\perp}) = \sum_{\mathbf{q}_m} \delta(\mathbf{k}'_{\perp} - \mathbf{k}_{\perp} + \mathbf{q}_m) \quad (14)$$

denotes the delta function for two-dimensional transverse momenta up to a reciprocal lattice vector, \mathbf{q}_m , of the emitter array. This describes the Bragg scattering of emitted light.

Equation (13) for the dressed photon propagator resembles the input-output relation Eq. (2), as it is given by the bare propagator in the absence of emitters, plus a matter contribution that describes the emission of light by the photon-dressed emitters. In fact, the set of Eqs. (8) to (11) and (13) reproduces the linear optical response of the system given by Eqs. (2) and (4) obtained from the master equation using the Markovian approximation, which in the present formalism corresponds to setting $\omega = \omega_e$ in the self-energy. In this limit, our diagrammatic theory recovers the known expressions for the transmission and reflection amplitudes, by propagating an initial single-photon plane wave state using the single-photon Green's function Eq. (13) (see Appendix B).

III. PHOTON-PHOTON INTERACTIONS

We now proceed to show how our formalism can describe non-linear effects quite naturally in terms of the scattering of dressed emitters. The Bethe-Salpeter equation for the scattering matrix of two dressed emitters is shown in Fig. 3a, where only ladder diagrams are non-zero since we consider only two photons [36]. As expressed in Eq. (7), the local onsite interaction does not carry a dependence on the momenta of the interacting excitations, which makes it possible to solve the Bethe-

Salpeter equation algebraically as $\mathcal{T} = U/[1 - U\Pi]$. Taking the limit $U \rightarrow \infty$ to describe that maximally one excitation is possible per emitter then yields

$$\mathcal{T}(\mathbf{K}_{\perp}, \Omega) = -\frac{1}{\Pi(\mathbf{K}_{\perp}, \Omega)}, \quad (15)$$

where

$$\Pi(\mathbf{K}_{\perp}, \Omega) = ia^2 \int \frac{d\omega}{2\pi} \int_{BZ} \frac{d^2 q_{\perp}}{(2\pi)^2} \mathcal{G}_{\bar{x}}^{(1)}(\mathbf{q}_{\perp}, \omega) \times \mathcal{G}_{\bar{x}}^{(1)}(\mathbf{K}_{\perp} - \mathbf{q}_{\perp}, \Omega - \omega) \quad (16)$$

is the pair propagator for two dressed excitations with total momentum $\mathbf{K}_{\perp} = \mathbf{k}_{\perp,1} + \mathbf{k}_{\perp,2}$ and total energy $\Omega = \omega_1 + \omega_2$. Taking $\Sigma(\mathbf{k}_{\perp}, \omega) \approx \Sigma(\mathbf{k}_{\perp}, \omega_e)$ (corresponding to the Markov approximation in a master equation approach) allows one to evaluate the frequency integral analytically, which yields the simple and intuitive expression

$$\Pi(\mathbf{K}_{\perp}, \Omega) = a^2 \int_{BZ} \frac{d^2 q_{\perp}}{(2\pi)^2} \frac{1}{\Omega - 2\omega_e - \Sigma(\mathbf{q}_{\perp}) - \Sigma(\mathbf{K}_{\perp} - \mathbf{q}_{\perp})} \quad (17)$$

for the pair propagator. With this relation and using the self-energy Eq. (11), the integral in Eq. (15) is readily evaluated numerically. Figure 4 shows the resulting scattering matrix for a lattice spacing of $a = 0.6\lambda_e$ and incident light on the reflection resonance of the array (in the figure $\gamma = d^2\omega_e^3/6\pi\epsilon_0\hbar c^3$ is the single-emitter decay rate). It can be seen that both its magnitude and phase vary only weakly across the Brillouin zone. It may thus be assumed constant around small transverse momenta of the incident light, which can be used to simplify calculations of the photon dynamics, as we shall discuss in the next section. Physically, this approximation corresponds to a short range on-site interaction between the dressed excitations. A similar diagrammatic approach for describing the propagation and scattering of polaritons in a Bose-Einstein condensate was developed in Refs. [51, 52].

IV. TWO-PHOTON DYNAMICS

Having solved the scattering problem of two dressed emitters, we are now ready to analyze the non-linear two-photon dynamics of the emitter array using our Green's function formalism. To this end, we need a connection between the Green's functions and the wave function of the photons. The time-dependent Green's function yields the evolution of an n -particle wave function $\Psi^{(n)}(\mathbf{r}^{(n)}, t')$

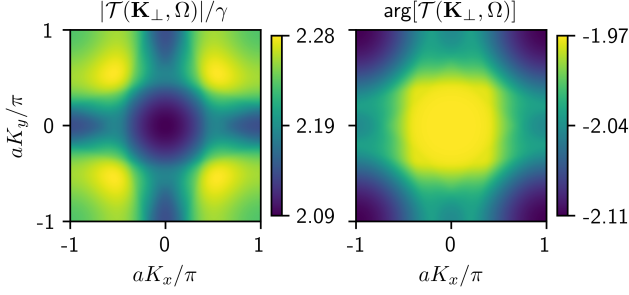


Figure 4. The absolute value and phase of $\mathcal{T}(\mathbf{K}_\perp, \Omega)$ is plotted as a function of momentum, with the frequency set to the single-photon reflection resonance $\Omega = 2(\omega_e + \tilde{\Delta}_0)$, and the lattice spacing $a = 0.6\lambda_e$.

of n positions $\mathbf{r}^{(n)} = (\mathbf{r}_1, \dots, \mathbf{r}_n)$ to a later time $t > t'$ as [37]

$$\begin{aligned} \Psi^{(n)}(\mathbf{r}^{(n)}, t) &= \int d^3r^{(n)'} G^{(n)}(\mathbf{r}^{(n)}, \mathbf{r}^{(n)'}, t - t') \Psi^{(n)}(\mathbf{r}^{(n)'}, t'). \end{aligned} \quad (18)$$

Equivalently, the Fourier transform, $G^{(n)}(\mathbf{k}^{(n)}, \mathbf{k}^{(n)'}, \omega)$, of the n -particle time-ordered Green's function $G^{(n)}(\mathbf{r}^{(n)}, \mathbf{r}^{(n)'}, t - t')$ describes the evolution from some initial momenta $\mathbf{k}^{(n)'}$ to some outgoing momenta $\mathbf{k}^{(n)}$ at a given total energy $\hbar\omega$. In the present case, we thus need the two-photon Green's function shown

$$\begin{aligned} \psi^{(2)}(\mathbf{k}_{\perp,1}, \mathbf{k}_{\perp,2}, z_1, z_2) &= 2\delta(\mathbf{k}_{\perp,1})\delta(\mathbf{k}_{\perp,2})(e^{ikz_1} - e^{ik|z_1|})(e^{ikz_2} - e^{ik|z_2|}) \\ &+ \frac{a^2}{2\pi^2}\delta(\mathbf{k}_{\perp,1} + \mathbf{k}_{\perp,2})\mathcal{T}(\mathbf{0}, \Omega) \frac{\tilde{\Gamma}_{\mathbf{k}_{\perp,1}}\tilde{\Gamma}_{\mathbf{k}_{\perp,2}}/\tilde{\Gamma}_0^2}{2\tilde{\Delta}_0 - \tilde{\Delta}_{\mathbf{k}_{\perp,1}} - \tilde{\Delta}_{\mathbf{k}_{\perp,2}} + i(\tilde{\Gamma}_{\mathbf{k}_{\perp,1}} + \tilde{\Gamma}_{\mathbf{k}_{\perp,2}})} e^{ik_z(|z_1| + |z_2|)} \\ &\times \left(\theta(d_2 - d_1) e^{i(\tilde{\Delta}_0 - \tilde{\Delta}_{\mathbf{k}_{\perp,1}}) - \tilde{\Gamma}_{\mathbf{k}_{\perp,1}}}(d_2 - d_1)/c} + 1 \leftrightarrow 2 \right) \end{aligned} \quad (19)$$

away from the emitter array, where the evanescent field can be neglected. Here, the total energy is $\Omega = 2\omega$ and we have removed an overall phase of $e^{-i\Omega t}$. Furthermore, $d_i = \frac{k}{k_{z,i}}|z_i|$, with the longitudinal momentum of each photon given by $k_{z,i} = \sqrt{k^2 - k_{\perp,i}^2}$, is the distance that a photon has propagated from the array for a given z_i and transverse momentum $\mathbf{k}_{\perp,i}$, see Fig. 5. This expression lets us quantify the essential mechanisms of the correlated photon interaction with the emitter array. The first line is non-zero only for $z < 0$ and accounts for the perfect linear reflection of the incident photons, while the remaining terms describe the nonlinear contribution to the induced photon field that is emitted symmetrically from the array in the positive and negative z -direction, with

diagrammatically in Fig. 3b, which consists of a term describing free propagation and an interaction term. Two incident photons are converted to dressed emitter excitations, which can propagate within the array, interact locally at a given site, and are subsequently emitted in the outgoing channel.

Using the scattering matrix, obtained in Eq. (15), we can now analyze the correlated scattering dynamics of incident light as determined by the two-photon Green's function shown in Fig. 3b (see Appendix C). It is used here to propagate an incident uncorrelated single-mode two-photon state $\Psi_{\text{in}}^{(2)}(\mathbf{k}_1\nu_1, \mathbf{k}_2\nu_2) = \Psi_{\text{in}}^{(1)}(\mathbf{k}_1, \nu_1)\Psi_{\text{in}}^{(1)}(\mathbf{k}_2, \nu_2)$. To this end, we evaluate the transverse integral in Eq. (18) in momentum space (\mathbf{k}_\perp) but choose a real-space representation along the z -axis, orthogonal to the emitter array. The only nontrivial contribution to the integral stems from the polarization component, $\psi_{\text{in}}^{(1)}(\mathbf{k}) = \sum_\nu \hat{\mathbf{e}}_+^\dagger \hat{\mathbf{e}}_{\mathbf{k}\nu} \Psi_{\text{in}}^{(1)}(\mathbf{k}, \nu)$, that couples to the emitters, which we choose here to be right-circularly polarized, as mentioned above.

While the general solution is given in Appendix D, we discuss here a simplified expression for normally incident light, $\psi_{\text{in}}^{(1)}(\mathbf{k}) = \delta(\mathbf{k}_\perp)\delta(k_z - k)$, which is on resonance with the zero transverse momentum collective transition of a subwavelength array. That is, we take the energy of each of the two incoming photons to be $\omega = ck = \omega_e + \tilde{\Delta}_0$. In this case, taking the limit $t \rightarrow \infty$ such that all transient dynamics have died away, one obtains a compact expression for the scattered photons

an emission pattern that remarkably is given by a simple Lorentzian factor of the collective energies. This term shows that the transmitted light solely stems from the effective interaction between the emitters, with a transmission amplitude that is proportional to the \mathcal{T} -matrix of the dressed emitter excitations.

While the linear response to single photons preserves the transverse momentum $\mathbf{k}_\perp = \mathbf{0}$, due to the suppression of Bragg scattering in a subwavelength array, the nonlinearity opens a scattering channel and facilitates the correlated emission of photon-pairs with transverse momenta $\mathbf{k}_{\perp,1} = -\mathbf{k}_{\perp,2}$. In addition to the transverse correlation, the photons are emitted in spatially localized pairs along the longitudinal z -direction, as described by

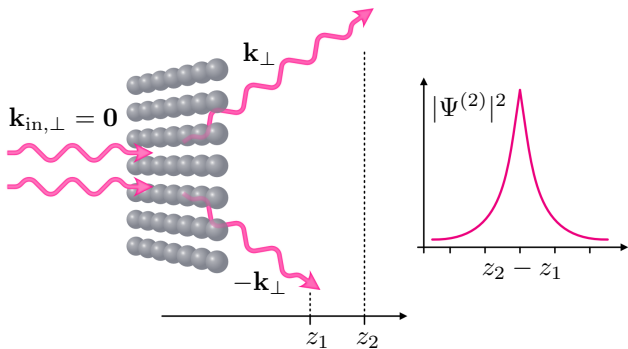


Figure 5. Photon-photon scattering leads to the correlated emission of photon pairs, whose localization length along the propagation direction of the incident light is determined by the collective decay rate of the array as illustrated in the figure.

the exponential factor $\theta(d_i - d_j)e^{-\tilde{\Gamma}_{\mathbf{k}_{\perp,j}}(d_i - d_j)/c}$. Here, d_i/c is the propagation time of the i 'th photon since its emission from the array, and accordingly, due to the step function $\theta(d_i - d_j)$, it is the decay rate $\tilde{\Gamma}_{\mathbf{k}_{\perp,j}}$ of the last emitted photon that defines the localization length of the photon pair (see Fig. 5 for the case of normal incidence photons). This is intuitively clear as the second photon simply decays according to the single-excitation lifetime of the collective mode corresponding to its momentum. This exponential localization of two photons represents a three-dimensional free-space analogue of so-called photon bound states that appear in waveguide-QED settings, where they arise from the interaction of a single quantum emitter with photons that propagate one-dimensionally in a single transverse mode [53, 54]. In fact, transmission exclusively arises from such bound states that are symmetrically emitted to either the same or opposite sides of the array.

One can make the above analogy more explicit by considering a transversally localized incident photon mode and analyzing the outgoing photon flux in that mode. To be specific, we consider a Gaussian incident mode that can be well described within the paraxial approximation by a single-photon amplitude $\psi_{\text{in}}^{(1)}(\mathbf{k}) = \sqrt{2\pi}w_0e^{-w_0^2k_{\perp}^2/4}e^{ik_z z}$. We further assume that the spatial beam waist w_0 is sufficiently large to confine the mode function to small transverse momenta, such that we can approximate $\Sigma(\mathbf{k}_{\perp}) \approx \Sigma(\mathbf{0})$ and $\mathcal{T}(\mathbf{k}_{\perp}) \approx \mathcal{T}(\mathbf{0})$. Even for fairly small values of w_0 , this remains a good approximation due to the weak momentum dependence of the \mathcal{T} -matrix, illustrated in Fig. 4. With these simplifications, we can project the outgoing photon state onto the Gaussian mode and obtain for the transmitted two-photon probability ($z_1, z_2 > 0$) in the Gaussian mode (see Appendix D)

$$P_2(z_1, z_2) = \frac{a^4}{w_0^4} \frac{|\mathcal{T}(\mathbf{0}, \Omega)|^2}{\pi^2 \tilde{\Gamma}_0^2} e^{-2\tilde{\Gamma}_0|z_2 - z_1|/c}, \quad (20)$$

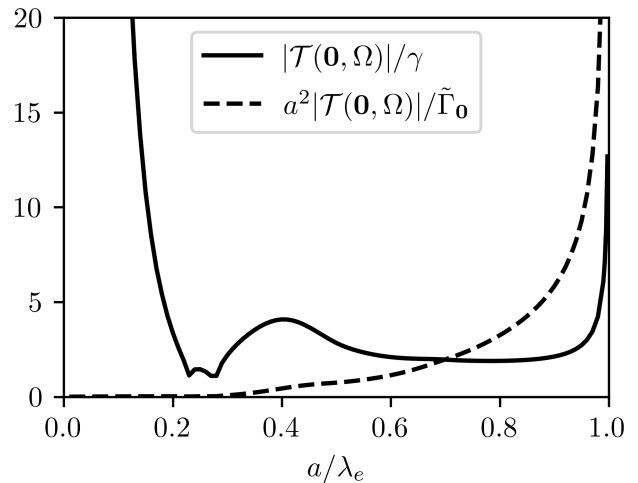


Figure 6. The absolute value of the \mathcal{T} -matrix in units of the single-emitter decay rate γ , as well as $a^2|\mathcal{T}(\mathbf{0}, \Omega)|/\tilde{\Gamma}_0$, are plotted at resonant driving, $\Omega = 2(\omega_e + \tilde{\Delta}_0)$, for different lattice constants a . The calculations show that while $|\mathcal{T}(\mathbf{0}, \Omega)|$ increases sharply near $a \sim 0$ and $a \sim \lambda_e$, the additional factors of a in $a^2|\mathcal{T}(\mathbf{0}, \Omega)|/\tilde{\Gamma}_0 \propto a^4|\mathcal{T}(\mathbf{0}, \Omega)|$ suppress the divergence at small a , but still allows for a strong nonlinearity when the emitters are resonantly spaced.

where we have again assumed resonant driving with $\omega = \omega_e + \tilde{\Delta}_0$. Hence, photons can only be transmitted in the form of an exponentially localized bound state, defined by the collective decay rate $\tilde{\Gamma}_0$. For $a < \lambda_e$, $\tilde{\Gamma}_0 = \frac{3\lambda_e^2}{4\pi a^2}\gamma \propto a^{-2}$, such that the bound state tightens with decreasing lattice spacing as the collective decay rate increases, while the overall flux of correlated photon pairs scales as $\sim a^8|\mathcal{T}(\mathbf{0}, \Omega)|^2$. The \mathcal{T} -matrix sharply increases around $a \sim 0$ and $a \sim \lambda$, resulting in a strong increase of photon-pair transmission as the lattice spacing approaches the transition wavelength of the quantum emitters. In Fig. 6 we plot the absolute value of the \mathcal{T} -matrix as well as $a^2|\mathcal{T}(\mathbf{0}, \Omega)|/\tilde{\Gamma}_0 \propto a^4|\mathcal{T}(\mathbf{0}, \Omega)|$, which is the a -dependent factor that enters our expressions. While the \mathcal{T} -matrix diverges at both $a = 0$, due to the emitters coalescing in a single point, and at $a = \lambda_e$, where they are at a resonant distance to each other, the full a -dependent factor vanishes for small a . Thus, nonlinear effects in the emitted light are suppressed for tight lattices, but grow strong for resonantly distributed emitters.

While the emerging bound states lead to strong photon bunching in the transmitted light, the interference with the linear response can likewise cause antibunching of reflected photons. An analogous calculation for the reflected light of an incident Gaussian mode yields the following simple expression for the two-photon temporal

correlation function (see Appendix D)

$$g^{(2)}(t) = \left| 1 + \frac{a^2}{2\pi w_0^2} e^{i(\Delta - \tilde{\Delta}_0) - \tilde{\Gamma}_0 t} \frac{\mathcal{T}(\mathbf{0}, \Omega)}{\Delta - \tilde{\Delta}_0 + i\tilde{\Gamma}_0} \right|^2 \quad (21)$$

where $\Delta = \omega - \omega_e$ is the detuning of the incident light. We see clearly how the reflected light correlations are determined by the geometric factor a^2/w_0^2 inversely proportional to the number of illuminated emitters, the emitter excitation scattering matrix, and the collective energies. In Fig. 7 we show the temporal correlations, $g^{(2)}(t)$, for different laser detunings across the reflection resonance of an array with $a = 0.6\lambda_e$. Despite the small lattice size and a relatively narrow beam waist of $w_0 = 2.5\lambda_e$, the linear response (inset of Fig. 7) matches that of an infinite lattice, which confirms the applicability of the paraxial approximation. More remarkably, the derived approximate expression Eq. (21) for the photon-photon correlations agrees very well with the numerical simulation of the master equation, Eqs. (2) and (4). The Green's function approach thus yields an accurate description and offers an intuitive understanding of nonlinear optical processes. While instantaneous correlations, $g^{(2)}(0)$, remains largely unaffected by the detuning, Δ , of the driving field, it has a significant effect on the temporal form of photon correlations, since it determines the relative phase between two-photon bound state and the linear contribution to the reflected light. As shown in Fig. 8, the degree of antibunching is largest around the reflection resonance (dashed line). Contrary to small systems of only few emitters [55, 56], deep subwavelength lattices show weak correlations due to the geometric factor a^2/w_0^2 , whereas photons become increasingly antibunched as the lattice spacing approaches λ_e and the \mathcal{T} -matrix increases (see Fig. 6). While the emitted light remains largely uncorrelated for most parameters in Fig. 8, under these conditions it, thus, becomes possible to convert an incident classical coherent field into pair-states of bound photons (in transmission) and antibunched light (in reflection) below the threshold $g^{(2)}(0) < 1/2$ [57] for nonclassical light.

V. CONCLUSION

In summary, we have developed a diagrammatic Green's function formalism to describe effective photon-photon interactions and the generation of correlated states of light in two-dimensional arrays of quantum emitters. Emitter excitations are treated as hardcore bosons in order to analyze their dynamics in terms of lattice polaritons, formed by hybridizing the two-dimensional collective excitations of the emitter array and the three-dimensional free-space electromagnetic field. Using Green's functions to study their interactions, we have obtained simple expressions for the optical response of the array and emerging photon-photon correlations in terms of the scattering matrix for interactions

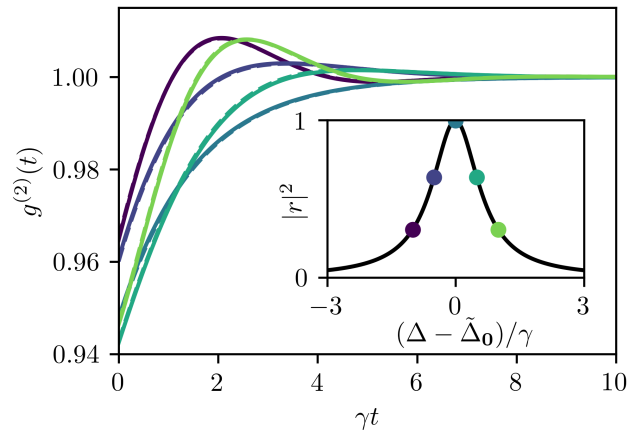


Figure 7. Two-photon correlation function $g^{(2)}(t)$ for an incident Gaussian beam with $w_0 = 2.5\lambda_e$, $a = 0.6\lambda_e$ and different detunings Δ , indicated by the coloured dots the inset. The analytical result Eq. (21) (solid lines) agrees well with the numerical simulation of a 15×15 array (dashed lines).

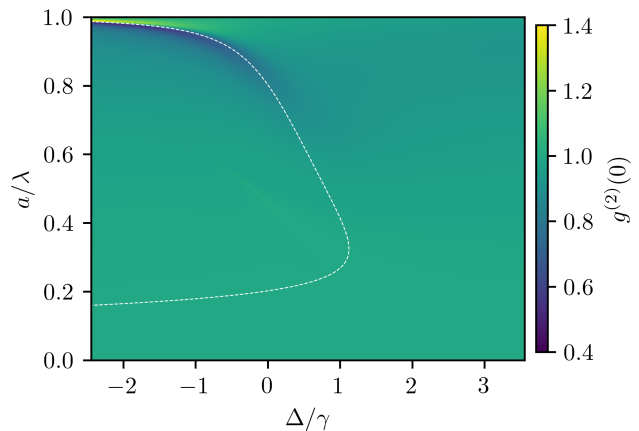


Figure 8. Equal-time two-photon correlations $g^{(2)}(0)$ as a function of the detuning Δ and the lattice spacing a . Strong antibunching occurs along the reflection resonance (white dashed line) near $a \sim 1$, consistent with the \mathcal{T} -matrix shown in Fig. 6.

between photon-dressed emitter excitations. The derivations show that correlations can be traced back to the formation of a two-photon bound state, whose size and contribution to the total state of the scattered light feature a simple dependence on the collective linewidth and the geometry of the array.

While we have focused here on the basic setup of a single planar square lattice of two-level quantum emitters, the outlined formalism can be readily extended to explore nonlinear processes arising from different types of emitter interactions [2, 28, 31, 58], multi-level atoms [59] and more complex geometries [60–65]. As we have shown, the discussed diagrammatic formalism provides an accurate yet simple description that offers intuitive insights into

the basic mechanisms for optical nonlinearities and effective photon-photon interactions, which could become useful in exploring applications of nonlinear processes in emitter arrays [28, 31, 66]. Importantly, it may be extended beyond the reach of numerical simulations by adapting established methods [36–38] for a systematic inclusion of the many-body effects arising from multiple interacting photons and dressed excitations.

VI. ACKNOWLEDGMENTS

We thank Ephraim Shahmoon, Lida Zhang, and Klaus Mølmer for valuable discussions. This work was supported by the Austrian Science Fund (Grant No. 10.55776/COE1) and the European Union (NextGenerationEU) and through the Horizon Europe ERC synergy grant SuperWave (grant no. 101071882).

Appendix A: The self-energy

The free-space electromagnetic dyadic Green's function can be written as

$$\mathbf{G}(\mathbf{k}_\perp, z, \omega) = \frac{i}{2k_z} \mathbf{Q}_{\text{sgn}(z)} e^{ik_z|z|}, \quad (\text{A1})$$

where $\mathbf{Q}_\pm = 1 - \hat{\mathbf{k}}\hat{\mathbf{k}}^\dagger$ is the projector onto the space of polarization vectors that is orthogonal to the wave vector $\mathbf{k} = (\mathbf{k}_\perp, \pm\sqrt{k^2 - k_\perp^2})$ of the forward and backward propagating light. Changing the integration variable in

Eq. (11) to $\omega_{\mathbf{k}}$, we have

$$\begin{aligned} \Sigma(\mathbf{k}_\perp, \omega) = & -i \frac{\mu_0}{2\pi\hbar a^2} \sum_{\mathbf{q}_m} \int_0^\infty d\omega_{\mathbf{k}} \omega_{\mathbf{k}}^2 \\ & \times \frac{\mathbf{d}^\dagger \text{Im}[\mathbf{G}(\mathbf{k}_\perp + \mathbf{q}_m, 0, \omega_{\mathbf{k}})] \mathbf{d}}{\omega - \omega_{\mathbf{k}} + i\eta}. \end{aligned} \quad (\text{A2})$$

Using $\mathbf{G}^*(\mathbf{r}_m, \mathbf{r}_n, \omega) = \mathbf{G}(\mathbf{r}_m, \mathbf{r}_n, -\omega^*)$ and $\lim_{|\omega| \rightarrow \infty} \omega^2 \mathbf{G}(\mathbf{r}_m, \mathbf{r}_n, \omega) = -\delta(\mathbf{r}_m - \mathbf{r}_n)$, one can evaluate the integral

$$\Sigma(\mathbf{k}_\perp, \omega) = -\frac{\mu_0 \omega_e^2}{\hbar a^2} \sum_{\mathbf{q}_m} \mathbf{d}^\dagger \mathbf{G}(\mathbf{k}_\perp + \mathbf{q}_m, 0, \omega) \mathbf{d}, \quad (\text{A3})$$

and obtain Eq. (12) from $\frac{1}{a^2} \sum_{\mathbf{q}_m} \mathbf{G}(\mathbf{k}_\perp + \mathbf{q}_m, 0, \omega) = N^{-1} \sum_{m,n} e^{i\mathbf{k} \cdot (\mathbf{r}_m - \mathbf{r}_n)} \mathbf{G}(\mathbf{r}_m, \mathbf{r}_n, \omega)$.

Appendix B: Single-photon transmission and reflection

The single-photon amplitude evolves as

$$\begin{aligned} \Psi^{(1)}(\mathbf{k}\nu, t) = & i \int \frac{d\omega}{2\pi} e^{-i\omega t} \\ & \times \sum_{\nu'} \int \frac{d^3 k'}{(2\pi)^3} G_{\tilde{\gamma}}^{(1)}(\mathbf{k}\nu, \mathbf{k}'\nu', \omega) \Psi_{\text{in}}^{(1)}(\mathbf{k}'\nu'). \end{aligned} \quad (\text{B1})$$

It is convenient to split $\Psi^{(1)}(\mathbf{k}\nu, t) = \Psi_0^{(1)}(\mathbf{k}\nu, t) + \Psi_{\text{sc}}^{(1)}(\mathbf{k}\nu, t)$ into a freely-evolving part, $\Psi_0^{(1)}$, and an induced component, $\Psi_{\text{sc}}^{(1)}$, corresponding to the first and second term in Eq. (13). The former gives $\Psi_0^{(1)}(\mathbf{k}\nu, t) = e^{-i\omega_{\mathbf{k}} t} \Psi_{\text{in}}^{(1)}(\mathbf{k}\nu)$. Only the projection, $\psi^{(1)}$, onto the polarization vector of the emitter transition is affected by the second term in Eq. (13). Here we choose right-circular polarization such that $\psi^{(1)}(\mathbf{k}, t) = \sum_\nu \hat{\mathbf{e}}_\perp^\dagger \hat{\mathbf{e}}_{\mathbf{k}\nu} \Psi^{(1)}(\mathbf{k}, \nu, t)$, as in Eq. (19). Using the second term in Eq. (13), the amplitude of the scattered light follows as

$$\begin{aligned} \psi_{\text{sc}}^{(1)}(\mathbf{k}, t) = & i \frac{c\tilde{\Gamma}_0}{\omega_e} \sqrt{\omega_{\mathbf{k}}} \sum_\nu \hat{\mathbf{e}}_+^\dagger \hat{\mathbf{e}}_{\mathbf{k}\nu} \hat{\mathbf{e}}_{\mathbf{k}\nu}^\dagger \hat{\mathbf{e}}_+ \int \frac{d\omega}{2\pi} e^{-i\omega t} \int \frac{d^3 k'}{2\pi} \delta_{\text{BZ}}(\mathbf{k}_\perp - \mathbf{k}'_\perp) \\ & \times \frac{1}{\omega + i\eta - \omega_{\mathbf{k}}} \frac{1}{\omega + i\eta - \omega_e - \Sigma(\mathbf{k}_\perp, \omega_e)} \frac{1}{\omega + i\eta - \omega_{\mathbf{k}'}} \sqrt{\omega_{\mathbf{k}'}} \psi_{\text{in}}^{(1)}(\mathbf{k}'), \end{aligned} \quad (\text{B2})$$

where we have used the periodicity of the self-energy in the reciprocal lattice momentum to evaluate Σ at the outgoing transverse momentum. Complex contour integration in ω gives

$$\psi_{\text{sc}}^{(1)}(\mathbf{k}, t) = -\frac{c\tilde{\Gamma}_0}{\omega_e} \sqrt{\omega_{\mathbf{k}}} \hat{\mathbf{e}}_+^\dagger \mathbf{Q} \hat{\mathbf{e}}_+ \int \frac{d^3 k'}{2\pi} \frac{\delta_{\text{BZ}}(\mathbf{k}_\perp - \mathbf{k}'_\perp)}{\omega_{\mathbf{k}'} - \omega_e - \Sigma(\mathbf{k}_\perp, \omega_e)} \frac{\sqrt{\omega_{\mathbf{k}'}} e^{-i\omega_{\mathbf{k}'} t}}{\omega_{\mathbf{k}} - \omega_{\mathbf{k}'} - i\eta} \psi_{\text{in}}^{(1)}(\mathbf{k}'), \quad (\text{B3})$$

where $\mathbf{Q} = \sum_{\nu} \hat{\mathbf{e}}_{\mathbf{k}\nu} \hat{\mathbf{e}}_{\mathbf{k}\nu}^{\dagger}$. The k'_z integration can be carried out for a monochromatic input field with $\omega = c|\mathbf{k}'|$ in the limit $t \rightarrow \infty$ to obtain for the total field

$$\psi^{(1)}(\mathbf{k}_{\perp} z) = e^{ik_z z} \psi_{\text{in}}^{(1)}(\mathbf{k}_{\perp}) - \frac{i\tilde{\Gamma}_0 \omega^2}{\omega_e c k_z} \frac{\hat{\mathbf{e}}_+^{\dagger} \mathbf{Q} \hat{\mathbf{e}}_+ e^{ik_z |z|}}{\omega - \omega_e - \Sigma(\mathbf{k}_{\perp}, \omega_e)} \sum_{\mathbf{q}_m} \psi_{\text{in}}^{(1)}(\mathbf{k}_{\perp} + \mathbf{q}_m), \quad (\text{B4})$$

up to an irrelevant factor $e^{-i\omega t}$ and where $k_z = \sqrt{(\omega/c)^2 - k_{\perp}^2}$. Assuming near-resonant driving ($\Delta \ll \omega_e$) and neglecting evanescent fields, we can identify $\Gamma_{\mathbf{k}_{\perp}} = \frac{\tilde{\Gamma}_0 \omega_e a^2}{c \text{Re}[k_z]} \hat{\mathbf{e}}_+^{\dagger} \mathbf{Q} \hat{\mathbf{e}}_+ = \frac{\mu_0 \omega_e^2}{\hbar} \mathbf{d}^{\dagger} \text{Im}[\mathbf{G}] \mathbf{d}$, which is related to the collective linewidth via $\tilde{\Gamma}_{\mathbf{k}_{\perp}} = \sum_{\mathbf{q}_m} \Gamma_{\mathbf{k}_{\perp} + \mathbf{q}_m}$. The total amplitude

$$\begin{aligned} \psi^{(1)}(\mathbf{k}_{\perp} z) &= e^{ik_z z} \psi_{\text{in}}^{(1)}(\mathbf{k}_{\perp}) \\ &- \frac{i\Gamma_{\mathbf{k}_{\perp}} e^{ik_z |z|}}{\Delta - \tilde{\Delta}_{\mathbf{k}_{\perp}} + i\tilde{\Gamma}_{\mathbf{k}_{\perp}}} \sum_{\mathbf{q}_m} \psi_{\text{in}}^{(1)}(\mathbf{k}_{\perp} + \mathbf{q}_m). \end{aligned} \quad (\text{B5})$$

thus, reduces to a sum of the incident wave and Bragg-scattered components that are symmetrically emitted from the array. When Bragg scattering is suppressed

at subwavelength lattice spacing, the sum only contains $\mathbf{q}_0 = \mathbf{0}$ and $\Gamma_{\mathbf{k}_{\perp}} = \tilde{\Gamma}_{\mathbf{k}_{\perp}}$, such that one recovers the known expressions

$$r = -\frac{i\tilde{\Gamma}_{\mathbf{k}_{\perp}}}{\Delta - \tilde{\Delta}_{\mathbf{k}_{\perp}} + i\tilde{\Gamma}_{\mathbf{k}_{\perp}}}, \quad (\text{B6})$$

and $t = 1 - r$ for the reflection and transmission coefficient, as readily obtained from the input-output formalism of Eqs. (2) to (4) [32].

Appendix C: The two-photon Green's function

The two-photon propagator can be written as

$$\begin{aligned} G_{\tilde{\gamma}}^{(2)}(\mathbf{k}_1 \nu_1 \omega_1, \mathbf{k}_2 \nu_2 \omega_2; \mathbf{k}'_1 \nu'_1 \omega'_1, \mathbf{k}'_2 \nu'_2 \omega'_2) & \\ &= - (2\pi)^2 \delta(\omega_1 - \omega'_1) \delta(\omega_2 - \omega'_2) G_{\tilde{\gamma}}^{(1)}(\mathbf{k}_1 \nu_1, \mathbf{k}'_1 \nu'_1 \omega_1) G_{\tilde{\gamma}}^{(1)}(\mathbf{k}_2 \nu_2, \mathbf{k}'_2 \nu'_2 \omega_2) \\ &- (2\pi)^2 \delta(\omega_1 - \omega'_2) \delta(\omega_2 - \omega'_1) G_{\tilde{\gamma}}^{(1)}(\mathbf{k}_1 \nu_1, \mathbf{k}'_2 \nu'_2 \omega_1) G_{\tilde{\gamma}}^{(1)}(\mathbf{k}_2 \nu_2, \mathbf{k}'_1 \nu'_1 \omega_2) \\ &- (2\pi)^3 \delta(\omega_1 + \omega_2 - \omega'_1 - \omega'_2) \delta_{\text{BZ}}(\mathbf{k}_{\perp,1} + \mathbf{k}_{\perp,2} - \mathbf{k}'_{\perp,1} - \mathbf{k}'_{\perp,2}) \\ &\times \mathcal{G}_{\tilde{\gamma}}^{(1)}(\mathbf{k}_1, \omega_1) g_{\mathbf{k}_1 \nu_1} \mathcal{G}_{\tilde{x}}^{(1)}(\mathbf{k}_{\perp,1}, \omega_1) \mathcal{G}_{\tilde{\gamma}}^{(1)}(\mathbf{k}_2, \omega_2) g_{\mathbf{k}_2 \nu_2} \mathcal{G}_{\tilde{x}}^{(1)}(\mathbf{k}_{\perp,2}, \omega_2) \\ &\times 2ia^2 \mathcal{T}(\mathbf{k}'_{\perp,1} + \mathbf{k}'_{\perp,2}, \omega'_1 + \omega'_2) \\ &\times \mathcal{G}_{\tilde{x}}^{(1)}(\mathbf{k}'_{\perp,1}, \omega'_1) g_{\mathbf{k}'_1 \nu'_1}^* \mathcal{G}_{\tilde{\gamma}}^{(1)}(\mathbf{k}'_1, \omega'_1) \mathcal{G}_{\tilde{x}}^{(1)}(\mathbf{k}'_{\perp,2}, \omega'_2) g_{\mathbf{k}'_2 \nu'_2}^* \mathcal{G}_{\tilde{\gamma}}^{(1)}(\mathbf{k}'_2, \omega'_2). \end{aligned} \quad (\text{C1})$$

The first two terms describe the free propagation of the dressed photons, while the third pertains to photon-photon scattering. The latter describes the conversion of two incident photons into dressed excitations via absorption, their scattering according to \mathcal{T} , and the subsequent emission of the two photons from the array (see also Fig. 3b). Although it contains many terms, the simple form of the \mathcal{T} -matrix and single-particle Green's functions permits to explicitly evolve monochromatic states, as we shall describe in more detail in the next section.

Appendix D: The two-photon wave function

Let us now use Eq. (C1) to time-evolve an incident single-mode two-photon state $\Psi_{\text{in}}^{(2)}(\mathbf{k}_1 \nu_1, \mathbf{k}_2 \nu_2) = \Psi_{\text{in}}^{(1)}(\mathbf{k}_1, \nu_1) \Psi_{\text{in}}^{(1)}(\mathbf{k}_2, \nu_2)$ according to

$$\begin{aligned} \Psi^{(2)}(\mathbf{k}_1 \nu_1, \mathbf{k}_2 \nu_2, t) &= \int \frac{d\omega_1 d\omega_2}{(2\pi)^2} e^{-i(\omega_1 + \omega_2)t} \\ &\sum_{\nu'_1, \nu'_2} \int \frac{d^3 k'_1 d^3 k'_2 d\omega'_1 d\omega'_2}{(2\pi)^6} \Psi_{\text{in}}^{(2)}(\mathbf{k}'_1 \nu'_1, \mathbf{k}'_2 \nu'_2) \\ &\times G_{\tilde{\gamma}}^{(2)}(\mathbf{k}_1 \nu_1 \omega_1, \mathbf{k}_2 \nu_2 \omega_2; \mathbf{k}'_1 \nu'_1 \omega'_1, \mathbf{k}'_2 \nu'_2 \omega'_2). \end{aligned} \quad (\text{D1})$$

Similar to the derivations in Appendix B, we can separate the amplitude into a linear part that is described by the first two lines on the right hand side of Eq. (C1) and a nonlinear part $\Psi_{\text{int}}^{(2)}$ that follows from the remaining terms. Projecting again onto the polarization component that couples to the emitters ($\hat{\mathbf{e}}_+$), we obtain

$$\begin{aligned}
\psi_{\text{int}}^{(2)}(\mathbf{k}_1, \mathbf{k}_2, t) &= \sum_{\nu_1, \nu_2} (\hat{\mathbf{e}}_+^\dagger \hat{\mathbf{e}}_{\mathbf{k}_1 \nu_1}) (\hat{\mathbf{e}}_+^\dagger \hat{\mathbf{e}}_{\mathbf{k}_2 \nu_2}) \Psi_{\text{int}}^{(2)}(\mathbf{k}_1 \nu_1, \mathbf{k}_2 \nu_2, t) \\
&= -2ia^2 \left(\frac{c\tilde{\Gamma}_0}{\omega_e} \right)^2 \sqrt{\omega_{\mathbf{k}_1} \omega_{\mathbf{k}_2}} \hat{\mathbf{e}}_+^\dagger \mathbf{Q}_1 \hat{\mathbf{e}}_+ \hat{\mathbf{e}}_+^\dagger \mathbf{Q}_2 \hat{\mathbf{e}}_+ \\
&\quad \times \int \frac{d^3 k'_1 d^3 k'_2}{(2\pi)^4} \delta_{\text{BZ}}(\mathbf{k}_{\perp,1} + \mathbf{k}_{\perp,2} - \mathbf{k}'_{\perp,1} - \mathbf{k}'_{\perp,2}) \sqrt{\omega_{\mathbf{k}'_1} \omega_{\mathbf{k}'_2}} \psi_{\text{in}}^{(2)}(\mathbf{k}'_1, \mathbf{k}'_2) \\
&\quad \times \int \frac{d\omega_1 d\omega_2}{(2\pi)^2} e^{-i(\omega_1 + \omega_2)t} \mathcal{G}_\gamma^{(1)}(\mathbf{k}_1, \omega_1) \mathcal{G}_\gamma^{(1)}(\mathbf{k}_2, \omega_2) \mathcal{G}_{\bar{x}}^{(1)}(\mathbf{k}_{\perp,1}, \omega_1) \mathcal{G}_{\bar{x}}^{(1)}(\mathbf{k}_{\perp,2}, \omega_2) \mathcal{T}(\mathbf{k}_{\perp,1} + \mathbf{k}_{\perp,2}, \omega_1 + \omega_2) \\
&\quad \times \int \frac{d\omega'_2}{2\pi} \mathcal{G}_\gamma^{(1)}(\mathbf{k}'_1, \omega_1 + \omega_2 - \omega'_2) \mathcal{G}_{\bar{x}}^{(1)}(\mathbf{k}'_{\perp,1}, \omega_1 + \omega_2 - \omega'_2) \mathcal{G}_\gamma^{(1)}(\mathbf{k}'_2, \omega'_2) \mathcal{G}_{\bar{x}}^{(1)}(\mathbf{k}'_{\perp,2}, \omega'_2),
\end{aligned} \tag{D2}$$

Carrying out the frequency integrals by complex contour integration and taking the limit $t \rightarrow \infty$ for monochromatic incident fields with frequencies ω_1 and ω_2 gives

$$\begin{aligned}
\psi_{\text{int}}^{(2)}(\mathbf{k}_1, \mathbf{k}_2) &= 2a^2 \left(\frac{c\tilde{\Gamma}_0}{\omega_e} \right)^2 \sqrt{\omega_{\mathbf{k}_1} \omega_{\mathbf{k}_2} \omega_1 \omega_2} \hat{\mathbf{e}}_+^\dagger \mathbf{Q}_1 \hat{\mathbf{e}}_+ \hat{\mathbf{e}}_+^\dagger \mathbf{Q}_2 \hat{\mathbf{e}}_+ \\
&\quad \times \mathcal{T}(\mathbf{k}_{\perp,1} + \mathbf{k}_{\perp,2}, \omega_1 + \omega_2) \frac{1}{\omega_1 + \omega_2 + i\eta - \omega_{\mathbf{k}_1} - \omega_{\mathbf{k}_2}} \\
&\quad \times \left(\frac{\omega_1 + \omega_2 - \omega_{\mathbf{k}_1} - \omega_{\mathbf{k}_2}}{\omega_1 + \omega_2 - \tilde{\omega}_{\mathbf{k}_{\perp,1}} - \tilde{\omega}_{\mathbf{k}_{\perp,2}}} + 1 \right) \frac{1}{(\omega_1 + \omega_2 - \omega_{\mathbf{k}_1} - \tilde{\omega}_{\mathbf{k}_{\perp,2}})(\omega_1 + \omega_2 - \tilde{\omega}_{\mathbf{k}_{\perp,1}} - \omega_{\mathbf{k}_2})} \\
&\quad \times \sum_{\mathbf{q}_m} \int \frac{d^2 q_\perp}{(2\pi)^2} \frac{1}{(\omega_1 - \tilde{\omega}_{\mathbf{k}'_{\perp,1}})(\omega_2 - \tilde{\omega}_{\mathbf{k}'_{\perp,2}})} \psi_{\text{in}}^{(2)}(\mathbf{k}'_{\perp,1}, \mathbf{k}'_{\perp,2}),
\end{aligned} \tag{D3}$$

where $\mathbf{k}'_{\perp,i} = (\mathbf{k}_{\perp,i} \pm \mathbf{q}_\perp + \mathbf{q}_m/2)$. Fourier transforming with respect to $k_{z,i}$ and neglecting evanescent-field contributions finally yields for the two-photon amplitude

$$\begin{aligned}
\psi_{\text{int}}^{(2)}(\mathbf{k}_{\perp,1} z_1, \mathbf{k}_{\perp,2} z_2) &= -2a^2 \frac{\mathcal{T}(\mathbf{k}_{\perp,1} + \mathbf{k}_{\perp,2}, \omega_1 + \omega_2)}{\Delta_1 + \Delta_2 - \tilde{\Delta}_{\mathbf{k}_{\perp,1}} - \tilde{\Delta}_{\mathbf{k}_{\perp,2}} + i(\tilde{\Gamma}_{\mathbf{k}_{\perp,1}} + \tilde{\Gamma}_{\mathbf{k}_{\perp,2}})} e^{i(k_{z,1}|z_1| + k_{z,2}|z_2|)} \\
&\quad \times \left(\theta(d_2 - d_1) e^{i(\Delta - \tilde{\Delta}_{\mathbf{k}_{\perp,1}}) - \tilde{\Gamma}_{\mathbf{k}_{\perp,1}}(d_2 - d_1)/c} + \theta(d_1 - d_2) e^{i(\Delta - \tilde{\Delta}_{\mathbf{k}_{\perp,2}}) - \tilde{\Gamma}_{\mathbf{k}_{\perp,2}}(d_1 - d_2)/c} \right) \\
&\quad \times \sum_{\mathbf{q}_m} \int \frac{d^2 q_\perp}{(2\pi)^2} \frac{\Gamma_{\mathbf{k}_{\perp,1}}/a^2}{\Delta_1 - \tilde{\Delta}_{\mathbf{k}'_{\perp,1}} + i\tilde{\Gamma}_{\mathbf{k}'_{\perp,1}}} \frac{\Gamma_{\mathbf{k}_{\perp,2}}/a^2}{\Delta_2 - \tilde{\Delta}_{\mathbf{k}'_{\perp,2}} + i\tilde{\Gamma}_{\mathbf{k}'_{\perp,2}}} \psi_{\text{in}}^{(2)}(\mathbf{k}'_{\perp,1}, \mathbf{k}'_{\perp,2}),
\end{aligned} \tag{D4}$$

where $k_{z,i} = \sqrt{(\omega_i/c)^2 - k_{\perp,i}^2}$ and $d_i = \frac{k}{k_{z,i}} |z_i|$. Considering normal-incident plane wave fields, $\psi_{\text{in}}^{(1)}(\mathbf{k}_i) = \delta(\mathbf{k}_{\perp,i}) \delta(k_{z,i} - \omega_i/c)$ and omitting Bragg scattering for subwavelength arrays, one arrives at Eq. (19). Likewise, choosing a broad Gaussian beam, $\psi_{\text{in}}^{(1)}(\mathbf{k}_i) = \phi_G(\mathbf{k}_i) = \sqrt{2\pi} w_0 e^{-w_0^2 k_{\perp,i}^2/4} e^{ik_{z,i} z}$, and projecting $\psi^{(2)}$ onto the same Gaussian mode

$$\begin{aligned}
\psi_G^{(2)}(z_1, z_2) &= \int \frac{d^2 k_{\perp,1} d^2 k_{\perp,2}}{(2\pi)^4} \phi_G^*(\mathbf{k}_{\perp,1} z_1) \phi_G^*(\mathbf{k}_{\perp,2} z_2) \\
&\quad \times \psi^{(2)}(\mathbf{k}_{\perp,1} z_1, \mathbf{k}_{\perp,2} z_2)
\end{aligned} \tag{D5}$$

one can arrive at Eq. (20) via

$$P_2(z_1, z_2) = \left| \psi_G^{(2)}(z_1, z_2) \right|^2 \tag{D6}$$

by taking $z_1, z_2 > 0$. There, the overlap between $\psi^{(1)}(\mathbf{k}_{\perp,i} z_i)$ and $\phi_G(\mathbf{k}_{\perp,i} z_i)$ is zero, when the Gaussian mode function is confined to small transverse momenta, such that we can approximate $\Sigma(\mathbf{k}_\perp) \approx \Sigma(\mathbf{0})$, resulting in the beam being fully reflected, and P_2 only containing the nonlinearly transmitted contribution. Analogously, one can arrive at Eq. (21) via

$$g^{(2)}(t) = \left| \frac{\psi_G^{(2)}(z_2 - z_1 = ct)}{2(\psi_G^{(1)})^2} \right|^2 \tag{D7}$$

Here, we exploit the fact that $\psi_G^{(2)}(z_1, z_2)$ only depends on the relative distance traveled by the photons, $|z_2 - z_1|$, to replace it with relative propagation time ct . This is due to the fact that $\psi_G^{(1)}$ is independent of z , as the z -

dependent phase of $\psi^{(1)}$ cancels with that of ϕ_G . Finally, the factor of 2 in the denominator comes from the fact that the two non-interacting diagrams of Fig. 3b contribute equally to the linear part of $\psi_G^{(2)}(z_1, z_2)$.

-
- [1] J. Rui, D. Wei, A. Rubio-Abadal, S. Hollerith, J. Zeiher, D. M. Stamper-Kurn, C. Gross, and I. Bloch, A subradiant optical mirror formed by a single structured atomic layer, *Nature* **583**, 369 (2020).
- [2] K. Srakaew, P. Weckesser, S. Hollerith, D. Wei, D. Adler, I. Bloch, and J. Zeiher, A subwavelength atomic array switched by a single Rydberg atom, *Nature Physics* **19**, 714 (2023).
- [3] G. Kestler, K. Ton, D. Filin, C. Cheung, P. Schneeweiss, T. Hoinkes, J. Volz, M. Safronova, A. Rauschenbeutel, and J. Barreiro, State-Insensitive Trapping of Alkali-Earth Atoms in a Nanofiber-Based Optical Dipole Trap, *PRX Quantum* **4**, 040308 (2023).
- [4] D. Lechner, R. Pennetta, M. Blaha, P. Schneeweiss, A. Rauschenbeutel, and J. Volz, Light-Matter Interaction at the Transition between Cavity and Waveguide QED, *Physical Review Letters* **131**, 103603 (2023).
- [5] X. Luan, J.-B. Béguin, A. P. Burgers, Z. Qin, S.-P. Yu, and H. J. Kimble, The Integration of Photonic Crystal Waveguides with Atom Arrays in Optical Tweezers, *Advanced Quantum Technologies* **3**, 2000008 (2020).
- [6] S.-P. Yu, J. A. Muniz, C.-L. Hung, and H. J. Kimble, Two-dimensional photonic crystals for engineering atom-light interactions, *Proceedings of the National Academy of Sciences* **116**, 12743 (2019).
- [7] C. Louca, A. Genco, S. Chiavazzo, T. P. Lyons, S. Randerson, C. Trovatiello, P. Claronino, R. Jayaprakash, X. Hu, J. Howarth, K. Watanabe, T. Taniguchi, S. Dal Conte, R. Gorbachev, D. G. Lidzey, G. Cerullo, O. Kyriienko, and A. I. Tartakovskii, Interspecies exciton interactions lead to enhanced nonlinearity of dipolar excitons and polaritons in MoS2 homobilayers, *Nature Communications* **14**, 3818 (2023).
- [8] B. Datta, M. Khatoniar, P. Deshmukh, F. Thouin, R. Bushati, S. De Liberato, S. K. Cohen, and V. M. Menon, Highly nonlinear dipolar exciton-polaritons in bilayer MoS2, *Nature Communications* **13**, 6341 (2022).
- [9] T. Stolz, H. Hegels, M. Winter, B. Röhr, Y.-F. Hsiao, L. Husel, G. Rempe, and S. Dürr, Quantum-Logic Gate between Two Optical Photons with an Average Efficiency above 40%, *Physical Review X* **12**, 021035 (2022).
- [10] N. Stiesdal, H. Busche, K. Kleinbeck, J. Kumlin, M. G. Hansen, H. P. Büchler, and S. Hofferberth, Controlled multi-photon subtraction with cascaded Rydberg superatoms as single-photon absorbers, *Nature Communications* **12**, 4328 (2021).
- [11] X.-L. Chu, C. Papon, N. Bart, A. D. Wieck, A. Ludwig, L. Midolo, N. Rotenberg, and P. Lodahl, Independent Electrical Control of Two Quantum Dots Coupled through a Photonic-Crystal Waveguide, *Physical Review Letters* **131**, 033606 (2023).
- [12] M. Zanner, T. Orell, C. M. F. Schneider, R. Albert, S. Oleschko, M. L. Juan, M. Silveri, and G. Kirchmair, Coherent control of a multi-qubit dark state in waveguide quantum electrodynamics, *Nature Physics* **18**, 538 (2022).
- [13] C. Gross and I. Bloch, Quantum simulations with ultracold atoms in optical lattices, *Science* **357**, 995 (2017).
- [14] H. Yu, G.-B. Liu, J. Tang, X. Xu, and W. Yao, Moiré excitons: From programmable quantum emitter arrays to spin-orbit-coupled artificial lattices, *Science Advances* **3**, e1701696 (2017).
- [15] H. Baek, M. Brotons-Gisbert, Z. X. Koong, A. Campbell, M. Rambach, K. Watanabe, T. Taniguchi, and B. D. Gerardot, Highly energy-tunable quantum light from moiré-trapped excitons, *Science Advances* **6**, eaba8526 (2020).
- [16] E. C. Regan, D. Wang, E. Y. Paik, Y. Zeng, L. Zhang, J. Zhu, A. H. MacDonald, H. Deng, and F. Wang, Emerging exciton physics in transition metal dichalcogenide heterobilayers, *Nature Reviews Materials* **7**, 778 (2022).
- [17] R. J. Bettles, S. A. Gardiner, and C. S. Adams, Enhanced optical cross section via collective coupling of atomic dipoles in a 2D array, *Physical Review Letters* **116**, 103602 (2016).
- [18] A. Asenjo-Garcia, M. Moreno-Cardoner, A. Albrecht, H. J. Kimble, and D. E. Chang, Exponential improvement in photon storage fidelities using subradiance and "selective radiance" in atomic arrays, *Physical Review X* **7**, 031024 (2017).
- [19] Y. Solomons, R. Ben-Maimon, and E. Shahmoon, Universal Approach for Quantum Interfaces with Atomic Arrays, *PRX Quantum* **5**, 020329 (2024).
- [20] G. Facchinetti, S. D. Jenkins, and J. Ruostekoski, Storing Light with Subradiant Correlations in Arrays of Atoms, *Physical Review Letters* **117**, 243601 (2016).
- [21] J. Ruostekoski and J. Javanainen, Arrays of strongly coupled atoms in a one-dimensional waveguide, *Physical Review A* **96**, 033857 (2017).
- [22] M. T. Manzoni, M. Moreno-Cardoner, A. Asenjo-Garcia, J. V. Porto, A. V. Gorshkov, and D. E. Chang, Optimization of photon storage fidelity in ordered atomic arrays, *New Journal of Physics* **20**, 083048 (2018).
- [23] P.-O. Guimond, A. Grankin, D. V. Vasilyev, B. Vermersch, and P. Zoller, Subradiant Bell states in distant atomic arrays, *Physical Review Letters* **122**, 093601 (2019).
- [24] K. E. Ballantine and J. Ruostekoski, Optical Magnetism and Huygens' Surfaces in Arrays of Atoms Induced by Cooperative Responses, *Physical Review Letters* **125**, 143604 (2020).
- [25] K. E. Ballantine and J. Ruostekoski, Cooperative optical wavefront engineering with atomic arrays, *Nanophotonics* **10**, 1901 (2021).
- [26] K. E. Ballantine, D. Wilkowski, and J. Ruostekoski, Optical magnetism and wavefront control by arrays of strontium atoms, *Physical Review Research* **4**, 033242 (2022).
- [27] N. S. Baßler, M. Reitz, K. P. Schmidt, and C. Genes, Linear optical elements based on cooperative subwavelength emitter arrays, *Optics Express* **31**, 6003 (2023).
- [28] M. Moreno-Cardoner, D. Goncalves, and D. E. Chang,

- Quantum Nonlinear Optics Based on Two-Dimensional Rydberg Atom Arrays, *Physical Review Letters* **127**, 263602 (2021).
- [29] J. Perczel, J. Borregaard, D. E. Chang, H. Pichler, S. F. Yelin, P. Zoller, and M. D. Lukin, Topological Quantum Optics in Two-Dimensional Atomic Arrays, *Physical Review Letters* **119**, 023603 (2017).
- [30] A. Asenjo-Garcia, H. J. Kimble, and D. E. Chang, Optical waveguiding by atomic entanglement in multilevel atom arrays, *Proceedings of the National Academy of Sciences* **116**, 25503 (2019).
- [31] L. Zhang, V. Walther, K. Mølmer, and T. Pohl, Photon-photon interactions in Rydberg-atom arrays, *Quantum* **6**, 674 (2022).
- [32] E. Shahmoon, D. S. Wild, M. D. Lukin, and S. F. Yelin, Cooperative Resonances in Light Scattering from Two-Dimensional Atomic Arrays, *Physical Review Letters* **118**, 113601 (2017).
- [33] S. P. Pedersen, L. Zhang, and T. Pohl, Quantum nonlinear metasurfaces from dual arrays of ultracold atoms, *Physical Review Research* **5**, L012047 (2023).
- [34] I. Carusotto and C. Ciuti, Quantum fluids of light, *Reviews of Modern Physics* **85**, 299 (2013).
- [35] B. Schrinski and A. S. Sørensen, Polariton interaction in one-dimensional arrays of atoms coupled to waveguides, *New Journal of Physics* **24**, 123023 (2022).
- [36] A. L. Fetter and J. D. Walecka, *Quantum Theory of Many-Particle Systems* (McGraw-Hill, 1971).
- [37] H. Bruus and K. Flensberg, *Many-Body Quantum Field Theory in Condensed Matter Physics: An Introduction* (Oxford University Press, 2003).
- [38] A. A. Abrikosov, I. Dzyaloshinskii, L. P. Gorkov, and R. A. Silverman, *Methods of Quantum Field Theory in Statistical Physics* (Dover, New York, NY, 1975).
- [39] R. H. Lehmann, Radiation from an N-Atom System. I. General Formalism, *Physical Review A* **2**, 883 (1970).
- [40] P. Longo, P. Schmitteckert, and K. Busch, Few-Photon Transport in Low-Dimensional Systems: Interaction-Induced Radiation Trapping, *Physical Review Letters* **104**, 023602 (2010).
- [41] D. Roy, Correlated few-photon transport in one-dimensional waveguides: Linear and nonlinear dispersions, *Physical Review A* **83**, 043823 (2011).
- [42] H. Zheng and H. U. Baranger, Persistent Quantum Beats and Long-Distance Entanglement from Waveguide-Mediated Interactions, *Physical Review Letters* **110**, 113601 (2013).
- [43] A. V. Poshakinskiy and A. N. Poddubny, Biexciton-mediated superradiant photon blockade, *Physical Review A* **93**, 033856 (2016).
- [44] Y. Ke, A. V. Poshakinskiy, C. Lee, Y. S. Kivshar, and A. N. Poddubny, Inelastic Scattering of Photon Pairs in Qubit Arrays with Subradiant States, *Physical Review Letters* **123**, 253601 (2019).
- [45] C. Murray and T. Pohl, Quantum and Nonlinear Optics in Strongly Interacting Atomic Ensembles, in *Advances In Atomic, Molecular, and Optical Physics*, Vol. 65 (Elsevier, 2016) pp. 321–372.
- [46] O. Firstenberg, C. S. Adams, and S. Hofferberth, Nonlinear quantum optics mediated by Rydberg interactions, *Journal of Physics B: Atomic, Molecular and Optical Physics* **49**, 152003 (2016).
- [47] T. Kazimierczuk, D. Fröhlich, S. Scheel, H. Stolz, and M. Bayer, Giant Rydberg excitons in the copper oxide Cu₂O, *Nature* **514**, 343 (2014).
- [48] V. Walther, R. Johné, and T. Pohl, Giant optical nonlinearities from Rydberg excitons in semiconductor microcavities, *Nature Communications* **9**, 1309 (2018).
- [49] J. Gu, V. Walther, L. Waldecker, D. Rhodes, A. Raja, J. C. Hone, T. F. Heinz, S. Kéna-Cohen, T. Pohl, and V. M. Menon, Enhanced nonlinear interaction of polaritons via excitonic Rydberg states in monolayer WSe₂, *Nature Communications* **12**, 2269 (2021).
- [50] K. Orfanakis, S. K. Rajendran, V. Walther, T. Volz, T. Pohl, and H. Ohadi, Rydberg exciton-polaritons in a Cu₂O microcavity, *Nature Materials* **21**, 767 (2022).
- [51] A. Camacho-Guardian, K. K. Nielsen, T. Pohl, and G. M. Bruun, Polariton dynamics in strongly interacting quantum many-body systems, *Physical Review Research* **2**, 023102 (2020).
- [52] A. Camacho-Guardian, M. Bastarrachea-Magnani, T. Pohl, and G. M. Bruun, Strong photon interactions from weakly interacting particles, *Physical Review B* **106**, L081302 (2022).
- [53] J.-T. Shen and S. Fan, Strongly correlated multiparticle transport in one dimension through a quantum impurity, *Physical Review A* **76**, 062709 (2007).
- [54] S. Mahmoodian, G. Calajó, D. E. Chang, K. Hammerer, and A. S. Sørensen, Dynamics of Many-Body Photon Bound States in Chiral Waveguide QED, *Physical Review X* **10**, 031011 (2020).
- [55] L. A. Williamson, M. O. Borgh, and J. Ruostekoski, Superatom Picture of Collective Nonclassical Light Emission and Dipole Blockade in Atom Arrays, *Physical Review Letters* **125**, 073602 (2020).
- [56] A. Cidrim, T. S. do Espirito Santo, J. Schachenmayer, R. Kaiser, and R. Bachelard, Photon Blockade with Ground-State Neutral Atoms, *Physical Review Letters* **125**, 073601 (2020).
- [57] M. O. Scully and M. S. Zubairy, *Quantum Optics*, 1st ed. (Cambridge University Press, 1997).
- [58] O. A. Iversen and T. Pohl, Self-ordering of individual photons in waveguide QED and Rydberg-atom arrays, *Physical Review Research* **4**, 023002 (2022).
- [59] S. J. Masson, J. P. Covey, S. Will, and A. Asenjo-Garcia, Dicke Superradiance in Ordered Arrays of Multilevel Atoms, *PRX Quantum* **5**, 010344 (2024).
- [60] C. D. Parmee, K. E. Ballantine, and J. Ruostekoski, Spontaneous symmetry breaking in frustrated triangular atom arrays due to cooperative light scattering, *Physical Review Research* **4**, 043039 (2022).
- [61] M. Cech, I. Lesanovsky, and B. Olmos, Dispersionless subradiant photon storage in one-dimensional emitter chains, *Physical Review A* **108**, L051702 (2023).
- [62] V. Scheil, R. Holzinger, M. Moreno-Cardoner, and H. Ritsch, Optical Properties of Concentric Nanorings of Quantum Emitters, *Nanomaterials* **13**, 851 (2023).
- [63] R. Ben-Maimon, Y. Solomons, N. Davidson, O. Firstenberg, and E. Shahmoon, Quantum interfaces with multilayered superwavelength atomic arrays (2024), arxiv:2402.06839 [quant-ph].
- [64] E. Sierra, S. J. Masson, and A. Asenjo-Garcia, Dicke Superradiance in Ordered Lattices: Dimensionality Matters, *Physical Review Research* **4**, 023207 (2022).
- [65] O. Rubies-Bigorda and S. F. Yelin, Superradiance and subradiance in inverted atomic arrays, *Physical Review A* **106**, 053717 (2022).
- [66] T. L. Patti, D. S. Wild, E. Shahmoon, M. D. Lukin, and

S. F. Yelin, Controlling interactions between quantum

emitters using atom arrays, [Physical Review Letters](#) **126**, 223602 (2021).